Electron. Mater. Lett., Vol. 11, No. 2 (2015), pp. 236-240
DOI: 10.1007/s13391-014-4326-9

Doping a D-A Structural Polymer Based on Benzodithiophene and Triazoloquinoxaline for Efficiency Improvement of Ternary Solar Cells

Qianqian Sun,[1] Fujun Zhang,[1,*] Jiefeng Hai,[2] Jiangsheng Yu,[2] Hui Huang,[3] Feng Teng,[1,*] and Weihua Tang[2,*]

[1]Key Laboratory of Luminescence and Optical Information, Ministry of Education, Beijing Jiaotong University, Beijing, 100044, China
[2]Key Laboratory of Soft Chemistry and Functional Materials, Ministry of Education, Nanjing University of Science and Technology, Nanjing, 210094, China
[3]School of Electrical Engineering, Beijing Jiaotong University, Beijing, 100044, China

(received date: 8 October 2014 / accepted date: 25 October 2014 / published date: 10 March 2015)

A novel donor-acceptor (D-A) structural polymer PBDT-BTzQx-C12 consisting of benzodithiophene and triazoloquinoxaline units as donor and acceptor building blocks was synthesized. The PBDT-BTzQx-C12 was evaluated as complementary electron donor in polymer solar cells (PSCs) with poly(3-hexylthiophene) (P3HT) as electron donor and [6,6]-phenyl-C71-butyric acid methyl ester ($PC_{71}BM$) as electron acceptor. The power conversion efficiencies (PCEs) of PSCs were improved from 3.18% to 3.54% by doping 2 wt. % PBDT-BTzQx-C12, corresponding to an approximately 11% PCE improvement. The performance improvement of ternary PSCs should be attributed to the increase of photon harvesting and the optimized phase separation of active layers by doping D-A structural PBDT-BTzQx-C12.

Keywords: polymer solar cells, power conversion efficiency, ternary bulk heterojunction, atomic force microscopy

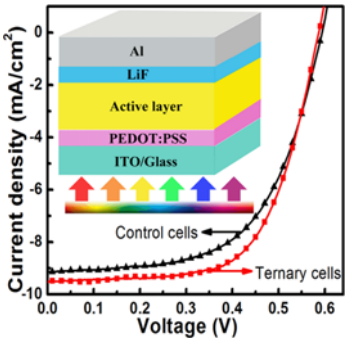

1. INTRODUCTION

Polymer solar cells (PSCs) have attracted much attention due to their unique properties of lightweight, flexible and cost-effective.[1-3] The bulk heterojunction with bi-continuous interpenetrated network has been proven to be most successful structure for obtaining high performance PSCs.[4-6] The donor-acceptor (D-A) structural polymers have attracted more and more attention due to the intramolecular charge carriers separation which is beneficial to exciton dissociation for obtaining high performance PSCs.[7] Benzo[1,2-b:4,5-b']dithiophene (BDT) is one of the most efficient donor building blocks for D-A structural polymers due to its high charge carrier mobility.[8] Quinoxaline derivatives have been widely used as the acceptor building blocks of D-A structural polymers because of their good electron withdrawing ability.[9]

*Corresponding author: fjzhang@bjtu.edu.cn
*Corresponding author: fteng@bjtu.edu.cn
*Corresponding author: whtang@njust.educ.cn

Recently, we successfully synthesized the D-A structural narrow band gap (~1.4 eV) polymer poly[4-(5-(4,8-bis (dodecyloxy)-4,8-dihydrobenzo[1,2-b:4,5-b']dithiophen-2-yl)-alt-5,8-bis-(thiophen-2-yl)-6,7-bis(3,4-bis(dodecyloxy) phenyl) -2-dodecyl-2H-[1,2,3]triazolo[4,5-g]quinoxaline] (PBDT-BTzQx-C12) with BDT as donor building block and TzQx as accepter building block.[10] The D-A structural polymer PBDT-BTzQx-C12 has two broad absorption ranges from 350 nm to 500 nm and from 600 nm to 900 nm, which has a complementary absorption spectra compared with that of poly(3-hexylthiophene) (P3HT).[11] It is known that ternary solar cells have been demonstrated as an effective strategy to improve the power conversion efficiency (PCE) by doping absorption spectral complementary materials.[12-14] The most reported complementary materials are narrow bang gap polymers to improve the performance of PSCs with P3HT as the electron donor.[15,16]

In this work, D-A structural polymer PBDT-BTzQx-C12 was doped into blend solutions of P3HT and [6,6]-phenyl-C71-butyric acid methyl ester ($PC_{71}BM$) with different doping ratios to improve the performance of PSCs. The

optimized PCE of ternary PSCs was about 3.54% with 2 wt. % PBDT-BTzQx-C12 doping ratio, corresponding to an approximately 11% PCE improvement compared with PSCs with P3HT:$PC_{71}BM$ as the active layer. The underlying reasons for the PCE improvement were discussed in the terms of photon harvesting and phase separation of active layers induced by different PBDT-BTzQx-C12 doping ratios.

2. EXPERIMENTAL PROCEDURE

The indium tin oxide (ITO) substrates with a sheet resistance of 15 Ω/square were cleaned consecutively in ultrasonic baths containing detergent, de-ioned water and ethanol. Then the cleaned ITO substrates were dried by nitrogen-gas and treated by UV-ozone for 10 min to further clean the substrates and increase the work function of ITO. The solution of poly-(3,4-ethylenedioxythiophene)-poly-(styrenesulfonate) (PEDOT:PSS) (purchased from H. C. Starck Co. Ltd.) was spin-coated onto the ITO substrates at 5000 round per min (rpm) for 40 s. Then PEDOT:PSS coated ITO substrates were dried in air at 120°C for 10 min. Polymer P3HT and fullerene derivative $PC_{71}BM$ were purchased from Luminescence Technology Corp and Organtec Materials Inc, respectively. All these materials were used as purchased. The PBDT-BTzQx-C12:$PC_{71}BM$ blends were dissolved in 1,2-dichlorobenzene (DCB) with different weight ratios (1:1, 1:2, 1:3, 1:4) keeping the PBDT-BTzQx-C12 concentration of 10 mg/mL. The ternary $P3HT_{(1-x)}$:PBDT-BTzQx-$C12_x$:$PC_{71}BM$ blends were dissolved in DCB with different PBDT-BTzQx-C12 doping weight ratios (x = 0, 0.01, 0.02, 0.03, 0.04). The blend solutions were spin-coated onto PEDOT:PSS coated ITO substrates to prepare the active layers in a high purity nitrogen filled glove box. And then a 1 nm LiF and 100 nm Al layers were deposited via thermal evaporation through a shadow mask in vacuum (10^{-4} Pa), which was monitored by a quartz crystal microbalance. The active area of each device is about 3.8 mm^2, which is defined by the overlap of the ITO anode and the Al cathode.

The current density-voltage (*J-V*) characteristics were measured using a Keithley 4200 semiconductor characterization system. AM 1.5 illumination at 100 mW/cm^2 was provided by an ABET Sun 2000 solar simulator. The external quantum efficiency (EQE) spectra were measured by a Zolix Solar Cell Scan 100. Absorption spectra were measured with a Shimadzu UV-3101 PC spectrophotometer. The morphologies of films were investigated by atomic force microscopy (AFM) using a multimode Nanoscope IIIa operated in tapping mode.

3. RESULTS AND DISCUSSION

The absorption spectra of P3HT and PBDT-BTzQx-C12 films were measured and are shown in the Fig. 1(a). There is an apparent absorption spectral complementary between PBDT-BTzQx-C12 and P3HT. Polymer P3HT has a relative strong absorption peak at 520 nm with two shoulders at 550 nm and 600 nm. The D-A structural polymer PBDT-BTzQx-C12 has two broad absorption ranges from 350 nm to 500 nm and from 600 nm to 900 nm, corresponding to two absorption peaks at 450 nm and 805 nm. The *J-V* curves of the cells based on PBDT-BTzQx-C12:$PC_{71}BM$ were investigated under AM 1.5 illumination at 100 mW/cm^2 with different donor:acceptor (D:A) doping ratios from 1:1 w/w to 1:4 w/w, as shown in the Fig. 1(b). The key photovoltaic parameters of PSCs were summarized and are shown in Fig. 1(b). The optimized PCE was 0.69% for the cells with D:A doping ratio of 1:2 w/w. The relatively low PCE may result from the lower EQE values in the whole spectral range, as shown in the Fig. 1(a). According to the absorption spectrum of D-A structural polymer PBDT-BTzQx-C12, it has a relative strong absorption in the longer wavelength range

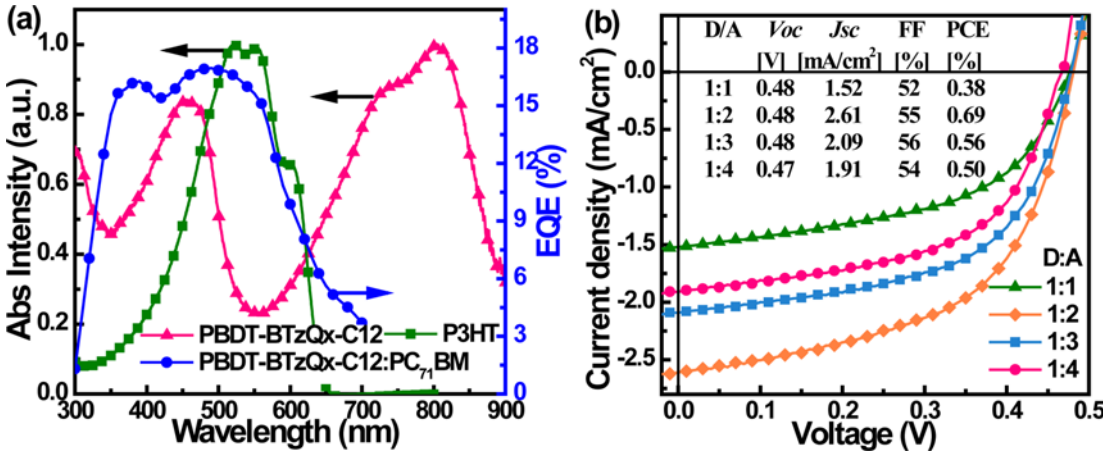

Fig. 1. (a) Absorption spectra of P3HT and PBDT-BTzQx-C12 films, EQE spectra of cells with D:A doping ratio of 1:2 w/w, (b) *J-V* curves of PSCs under AM 1.5 illumination at 100 mW/cm^2.

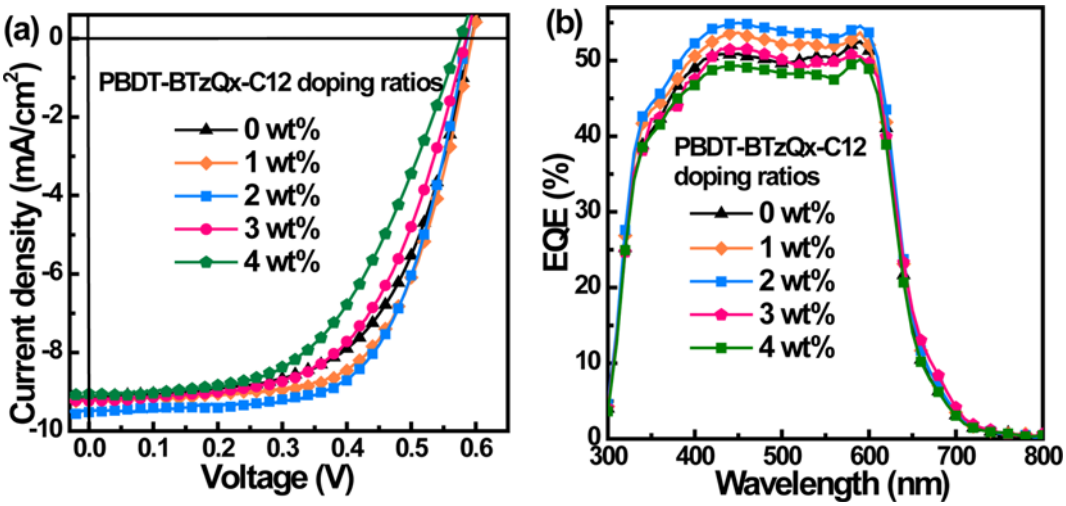

Fig. 2. (a) *J-V* characteristic curves of PSCs under AM 1.5 illumination at 100 mW/cm^2, (b) the EQE spectra of PSCs based on P3HT:$PC_{71}BM$ with different PBDT-BTzQx-C12 doping ratios.

from 600 nm to 900 nm, however, the EQE values are rather low in this longer wavelength range. It means that these photogenerated excitons in PBDT-BTzQx-C1 can't be dissociated into free charge carriers. Therefore, the performance of PSCs with PBDT-BTzQx-C1:$PC_{71}BM$ as the active layers is only related to the PBDT-BTzQx-C1 photon harvesting in shorter wavelength range.

A series of binary PSCs with P3HT:$PC_{71}BM$ (1:1) as the active layers (control cells) and ternary PSCs with $P3HT_{(1-x)}$:PBDT-BTzQx-$C12_x$:$PC_{71}BM$ (x = 0, 0.01, 0.02, 0.03, 0.04) as the active layers were fabricated to investigate the effect of PBDT-BTzQx-C12 doping ratios on performance of PSCs. The *J-V* curves of all the PSCs were measured under AM 1.5 illumination at 100 mW/cm^2 and are shown in Fig. 2(a). According to *J-V* curves, the key photovoltaic parameters of PSCs are summarized in Table 1. It is apparent that the PCE of PSCs can be improved by doping PBDT-BTzQx-C12 ratios less than 2 wt. % and then decreased along with increase of PBDT-BTzQx-C12 doping ratios. The PCE of control cells was about 3.18%, with short circuit current density (J_{sc}) of 9.13 mA/cm^2, open circuit voltage (V_{oc}) of 0.59 V and fill factor (FF) of 59%. For all the ternary PSCs, the V_{oc} was kept at 0.59 V with 0.01 V indeterminacy. The J_{sc} and FF were increased and then decreased along with the increase of PBDT-BTzQx-C12 doping ratios. The optimized PCE of ternary PSCs was 3.54% for the cells with 2 wt. % PBDT-BTzQx-C12 doping ratio, corresponding to an approximately 11% PCE improvement compared with the control cells.

Table 1. Key photovoltaic parameters of PSCs with different PBDT-BTzQx-C12 doping ratios.

Doping ratios	V_{oc} [V]	J_{sc} [mA/cm^2]	FF [%]	PCE [%]
0 wt. %	0.59	9.13	59	3.18
1 wt. %	0.59	9.21	64	3.48
2 wt. %	0.59	9.52	63	3.54
3 wt. %	0.59	9.23	57	3.10
4 wt. %	0.58	9.05	52	2.73

In order to further confirm the effect of PBDT-BTzQx-C12 doping ratios on performance of PSCs, EQE spectra of PSCs were measured and are shown in Fig. 2(b). The EQE spectral shape of ternary PSCs is very similar with that of control cells. It means that the contribution of PBDT-BTzQx-C12 in the longer wavelength on the performance improvement of PSCs can be ignored, which accords with the observed from PSCs with PBDT-BTzQx-C12:$PC_{71}BM$ as the active layer. The EQE values of ternary PSCs were increased and then decreased along with the increase of PBDT-BTzQx-C12 doping ratios in the wavelength range from 350 nm to 600 nm. The increased EQE values of ternary PSCs should be attributed to the contribution of PBDT-BTzQx-C12 on the photon harvesting, and exciton dissociation in the active layers. The EQE values of PSCs were decreased when the PBDT-BTzQx-C12 doping ratios were larger than 2 wt. %, which may be due to the relative decrease of P3HT content and the disordered interpenetrating networks of P3HT and $PC_{71}BM$ induced by doping PBDT-BTzQx-C12. This explanation can be supported from FF variation dependence on the PBDT-BTzQx-C12 doping ratios. It is known that the effective charge carrier transport and collection in the active layer results in a large FF and J_{sc}.[17] For the ternary PSCs, the FF and J_{sc} values were increased and then decreased along with the increase of PBDT-BTzQx-C12 doping ratios.

For the better understand the effect of PBDT-BTzQx-C12 doping ratios on the performance of PSCs, the morphology

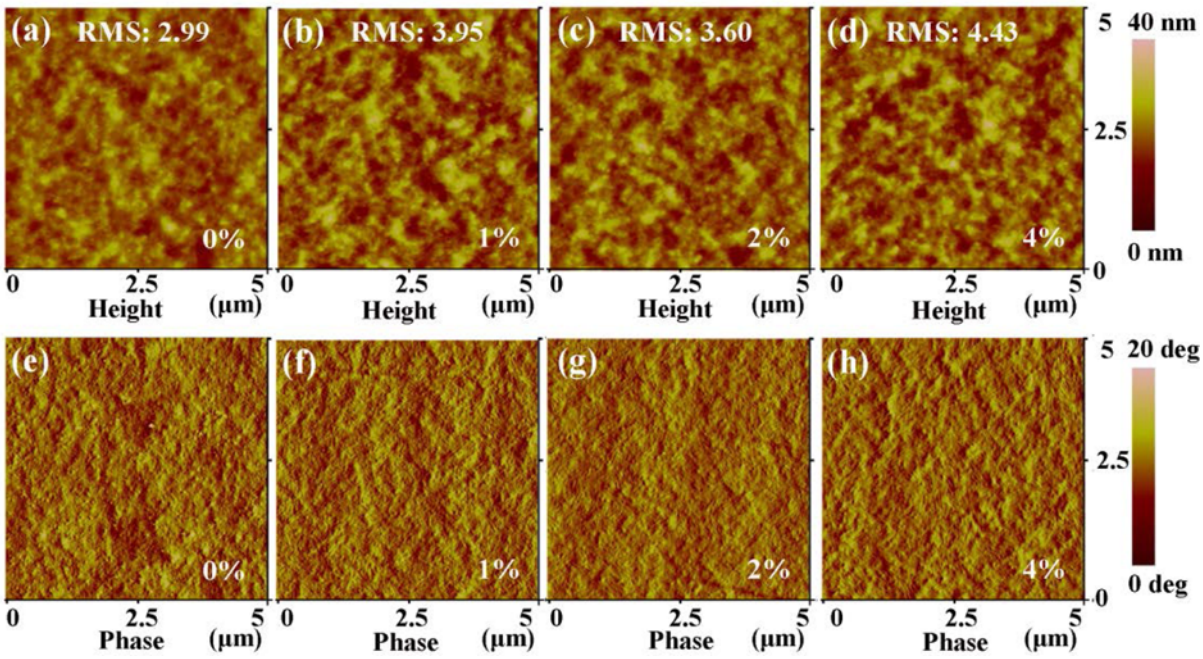

Fig. 3. AFM morphology images (a-c) and phase images (e-h) of active layers with different PBDT-BTzQx-C12 doping ratios.

and phase of active layers were measured by atomic force microscopy, as shown in the Fig. 3. The root-mean-square (RMS) surface roughness are evaluated about 2.99 nm, 3.95 nm, 3.60 nm, and 4.43 nm for the active layers with PBDT-BTzQx-C12 doping ratios at 0 wt. %, 1 wt. %, 2 wt. % and 4 wt. %, respectively. The relative phase images show an apparent increased phase separation trend along with increase of PBDT-BTzQx-C12 doping ratios. The more homogeneous phase distribution can be observed from the active layer with 2 wt. % PBDT-BTzQx-C12 doping ratio, which means that an ideal interpenetrating network can be formed for better exciton dissociation and charge transport in the active layer. The molecular aggregation trend becomes more apparent when the PBDT-BTzQx-C12 doping ratios are larger than 2 wt. %. It is apparent that the morphology and phase separation of ternary blend films can be adjusted by changing PBDTBTzQx-C12 doping ratios, which affects the exciton dissociation and charge carrier transport in the active layer.

4. CONCLUSIONS

In summary, the optimized PCE of ternary PSCs was 3.54% with 2 wt. % PBDT-BTzQx-C12 doping ratio, corresponding to an approximately 11% improvement compared with 3.18% PCE of the control cells. The effect of D-A structural polymer PBDT-BTzQx-C12 doping ratios on the performance of PSCs can be summarized: i) enhancing the photon harvesting in the wavelength range from 350 nm to 600 nm, ii) adjusting the morphology and phase of blend films for better exciton dissociation and charge carrier transport in the active layers. The ternary solar cells provide a very simple method to improve PCE of PSCs compared with tandem solar cells.

ACKNOWLEDGEMENTS

The authors wish to thank the Fundamental Research Funds for the Central Universities (2014JBZ017); National Natural Science Foundation of China (613770029); National Natural Foundation of Distinguished Young Scholars of China (61125505); Beijing Natural Science Foundation (2122050).

REFERENCES

1. F. J. Zhang, X. W. Xu, W. H. Tang, J. Zhang, Z. L. Zhuo, J. Wang, J. Wang, Z. Xu, and Y. S. Wang, *Sol. Energy Mater. Sol. Cells* **95**, 1785 (2011).
2. M. Ahmadi, K. Mirabbaszadeh, and M. Ketabchi, *Electron. Mater. Lett.* **9**, 729 (2013).
3. P.-H. Wang, H.-F. Lee, Y.-C. Huang, Y.-J. Jung, F.-L. Gong, and W.-Y. Huang, *Electron. Mater. Lett.* **10**, 767 (2014).
4. S. Ochiai, P. Kumar, K. Santhakumar, and P. K. Shin, *Electron. Mater. Lett.* **9**, 399 (2013).
5. J. M. Lee, B. H. Kwon, H. I. Park, H. Kim, M. G. Kim, J. S. Park, E. S. Kim, S. Yoo, D. Y. Jeon, and S. O. Kim, *Adv. Mater.* **25**, 2011 (2013).

6. L. Y. Lu, T. Xu, W. Chen, J. M. Lee, Z. Q. Luo, I. H. Jung, H. I. Park, S. O. Kim, and L. P. Yu, *Nano Lett.* **13**, 2365 (2013).
7. F. Y. Wu, D. J. Zha, L. Chen, and Y. W. Chen, *J. Polym. Sci. Pol. Chem.* **51**, 1506 (2013).
8. P. Sista, M. C. Biewer, and M. C. Stefan, *Macromol. Rapid Commun.* **33**, 9 (2012).
9. J. H. Kim, C. E. Song, H. U. Kim, I. N. Kang, W. S. Shin, M. J. Park, and D. H. Hwang, *J. Polym. Sci. Pol. Chem.* **51**, 4136 (2013).
10. J. F. Hai, W. Yu, B. F. Zhao, Y. Li, L. M. Yin, E. W. Zhu, L. Y. Bian, J. A. Zhang, H. B. Wu, and W. H. Tang, *Polym. Chem.* **5**, 1163 (2014).
11. T. Ameri, P. Khoram, J. Min, and C. J. Brabec, *Adv. Mater.* **25**, 4245 (2013).
12. Q. S. An, F. J. Zhang, L. L. Li, J. Wang, J. Zhang, L. Y. Zhou, and W. H. Tang, *ACS Appl. Mat. Interfaces* **6**, 6537 (2014).
13. J. S. Huang, T. Goh, X. K. Li, M. Y. Sfeir, E. A. Bielinski, S. Tomasulo, M. L. Lee, N. Hazari, and A. D. Taylor, *Nat. Photonics* **7**, 480 (2013).
14. Q. S. An, F. J. Zhang, L. L. Li, Z. L. Zhuo, J. Zhang, W. H. Tang, and F. Teng, *Phys. Chem. Chem. Phys.* **16**, 16103 (2014).
15. Q. S. An, F. J. Zhang, J. Zhang, W. H. Tang, Z. X. Wang, L. L. Li, Z. Xu, F. Teng, and Y. S. Wang, *Sol. Energy Mater. Sol. Cells* **118**, 30 (2013).
16. M. T. Dang, L. Hirsch, and G. Wantz, *Adv. Mater.* **23**, 3597 (2011).
17. B. B. Chen, X. F. Qiao, C. M. Liu, C. Zhao, H. C. Chen, K. H. Wei, and B. Hu, *Appl. Phys. Lett.* **102**, 193302 (2013).